THE CORRELATION BETWEEN STATIC INDENTATION EXPERIMENT AND ANALYTICAL MODEL FOR THE BEHAVIOR OF THE COMPOSITE LAMINATES SUBJECTED TO HIGH VELOCITY IMPACT

H. Shin, W. You, I. Kim*, S. Lee, S. Ha, and S. Cho
Department of Aerospace Engineering, Chungnam National University
220 Gung-Dong, Yuseong-Gu, Daejeon, Korea, 305-764
*Corresponding author(igkim@cnu.ac.kr)

Keywords: static indentation, high velocity impact, composite laminates, numerical finite element analysis

1 Introduction

The high-velocity impact such as bird strike, debris of engine fan blade, and a hailstorm, could cause delamination, surface spallation, penetration, and reduction of strength and stiffness of the structure [1]. The purpose of this study is the improvement of the finite element analysis model and the prediction of the behavior of composite laminates subjected to the high velocity impact by using the static indentation experiment results. In the static indentation experiment, the indentation energy was calculated from the load-displacement curve which was obtained from universal testing machine (model: INSTRON 5882). A finite element analytical program, LS-DYNA, was used to interpret the failure characteristics of the composite laminates during the static indentation. The correlation of the result between the static indentation experiment and the finite element model is investigated. Using this static indentation model, the penetration energy of composite laminates subjected to high velocity impact is predicted. In the high-velocity impact experiment, a steel ball is fired from a compressed air gun, and impact energy is calculated by the procedure of the load transfer from the steel ball to the specimen. In this experiment, the absorbed energy is calculated with using the initial velocity and the residual velocity after penetration. With considering high strain rate [2], the validity of the numerical analysis results are examined by comparing with the experiment results.

2 Experimental Procedures

The specimens used in this study are solid laminates made of graphite/epoxy prepreg (USN150B) with two kinds of $[45/0/-45/90]_{2S}$ and $[45/0/-45/90]_{3S}$, stacking sequences. The properties of Gr/Ep unidirectional laminates are presented in Table 1.

Table 1. Material properties of Gr/Ep (USN 150B)

Property	Symbol	Value
Elastic modulus	E_1	131GPa
	E_2	8.2GPa
	E_3	8.2GPa
Shear modulus	G_{12}	4.5GPa
	G_{13}	4.5GPa
	G_{13}	3.5GPa
Poisson's ratios	ν_{12}	0.28
	ν_{13}	0.28
	ν_{23}	0.47
Tensile strength	X_T	2,000MPa
	Y_T	61MPa
	Z_T	61MPa
Shear strength	S_{12}	70MPa
	S_{13}	70MPa
	S_{23}	40MPa
Thickness	T	0.141mm
Density	ρ	$1580k/m^3$

2.1 Static Indentation Experiment

The static indentation experimental set-up is shown in Fig. 1. The experiment is conducted by controlling the displacement of indentor to come down at a speed of 2.5mm/min. The specimen is placed on a steel fixture, and the load is applied to the specimen until penetrating the specimen by the UTM (Instron 5882). The size of the specimen is 87.5mm x 87.5mm, and all the edges are clamped by the steel fixture. The exposed circular area of the specimens is varied to examine the relation between the effective area and penetration energy. There are three kinds of specimen grouped by the diameter ratio (D/d) of the effective area to the indentor, and each D/d is 3, 4, and 5, respectively (D: the diameter of the effective area, d: the diameter of the indentor). The force-displacement curves by the data obtained from the indentation experiment are shown in Fig. 2. Each absorbed energy to penetrate the specimens is calculated from the force-displacement curves [3]. The maximum load becomes smaller as D/d ratio increases but absorbed energy is almost same independent of D/d ratio as shown in Fig. 2.

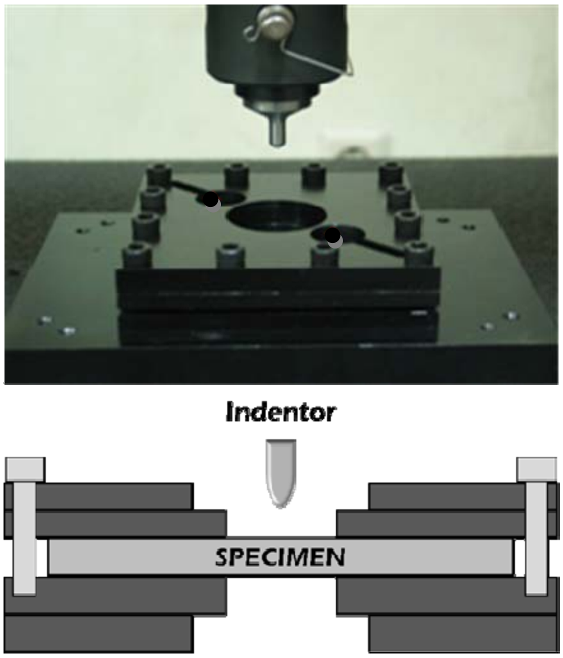

Fig. 1. Static indentation experimental set-up

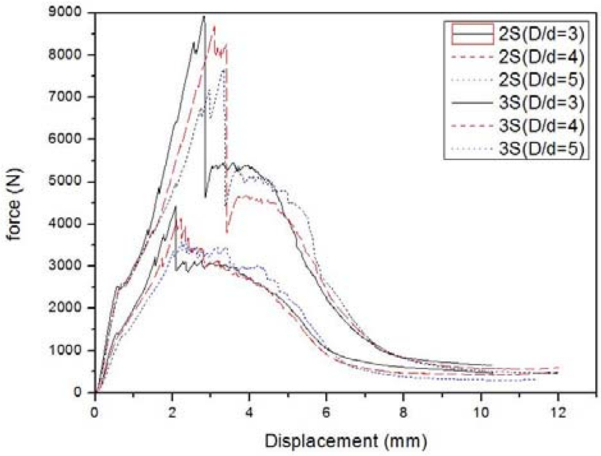

Fig. 2. Force-displacement curves
for the different D/d

2.2 High-Velocity Impact Experiment

The high-velocity impact facility consists of pressurized air tank, gun barrel, four magnetic sensors for measuring the steel ball velocity, supporting fixtures, and a signal acquisition system as shown in Fig. 3. The steel ball was fired from gun barrel by the compressed air, and the impact is transmitted to the specimen. The steel ball has a dimension of a 6.35 mm diameter (mass: 1.044 gram), and it is the same diameter as that used in the static indentation experiment. The specimens used in the high-velocity impact experiment are same as those used in the static indentation experiment. The AE sensor (UT-1000) is used to monitor the AE signal comes from impact damage and attached on the same location as the static indentation experiment [4]. The penetration energy is estimated using the velocity difference of steel ball between before/after perforating the specimen.

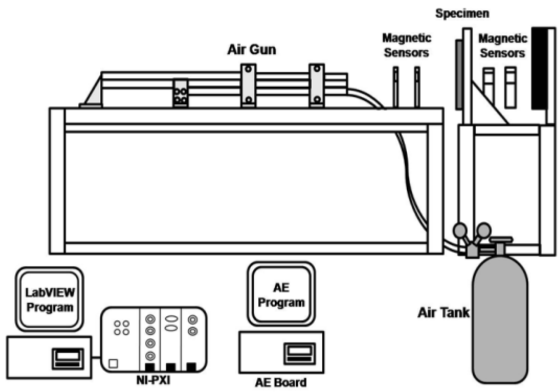

Fig. 3. High-velocity impact experimental set-up

2.3 Experiment Results

The comparisons of the penetration energy from the static indentation and the high-velocity impact experiment are presented in Table 2. The penetration energy of the static indentation experiment is less than that of the high-velocity impact experiment as shown Table 2. These difference mainly coms from the effect of the boundary condition as well as strain rate. Especially, strain rate affects the elastic modulus and the failure strain, and then it makes the penetration energy less in static indentation experiment. It seems that D/d ratio doesn't make much difference to the increase rate of penetration energy (%) as shown in Table 3.

Table 3. Comparison of the penetration energy of two penetration experiments

Lay up	D/d	Static indentation	High-velocity impact	Increase rate of penetration energy (%)
		Penetration energy (J)		
$[45/0/-45/90]_{2S}$	3	9.64	12.77	132
	4	10.30	13.98	136
	5	11.42	15.29	134
$[45/0/-45/90]_{3S}$	3	18.08	24.52	136
	4	19.57	26.55	136
	5	20.52	27.92	136

3 Numerical Analysis for Composite Materials

3.1 Finite Element Modeling

Using a commercial finite element analysis S/W(LS-DYNA), the behavior of the composite laminates by the static indentation was simulated. The finite element model was developed by using the nonlinear, explicit dynamic code. The finite element model is shown in Fig. 4.
The steel fixture was modeled in detail to make the proper boundary condition and was fully constrained like rigid body. The indentor was modeled as rigid body. For the boundary condition of the indentor, the displacements along the global axes x and y, and the rotations for the three global axes were constrained while the z axis downwards was allowed. To simulate the quasi-static analysis, the indentor was given the prescribed velocity which was much higher than that in actual experiment to reduce the computational run time.
The contact card (*CONTACT AUTOMATIC SURFACE TO SURFACE) was adopted between the indentor and the specimen.

3.2 Material Modeling

In this finite element analysis, as the steel fixture and the indentor, the specimen was modeled by using a shell element to reduce the computational run time. The composite failure model within LS-DYNA is the Chang-Chang (1987) model (*MAT 22, *MAT COMPOSITE DAMAGE). *MAT 22 provides various fiber and matrix failure modes solely due to in-plane stresses in unidirectional lamina. In this 2D failure model, the failure mode due to out-of-plane shear and normal stresses are neglected. While this card may be sufficient for composite structures under in-plane loading, it may be unable to capture transverse impact failures for which all six stress components are known to contribute to damage development [5].
In *MAT 22, five material parameters are used in the three failure criteria (the matrix cracking failure criteria, compression failure criteria, and the fiber breakage).

- S1, longitudinal tensile strength
- S2, transverse tensile strength
- S12, shear strength
- C2, transverse compressive strength
- α, nonlinear shear stress parameter

S1, S2, S12, and C2 are obtained from material strength measurement. α is defined by material shear stress-strain measurements. A more detailed description of *MAT 22 is provided in [6].

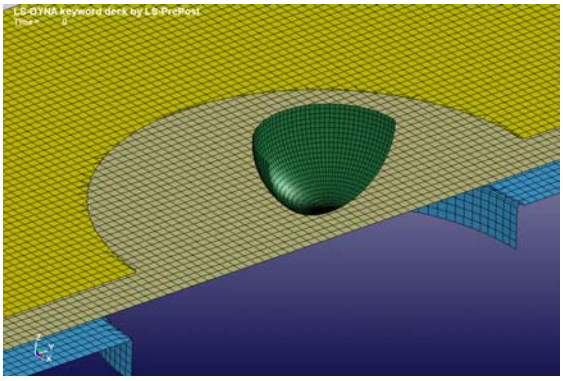

Fig. 4. The finite element model

4 Results and Discussion

In general, composite materials properties are randomly distributed around their mean value and it is reasonable to modify the material properties in the acceptable range. In this study, the original material properties of graphite/epoxy in Table 1 were used in the Analysis-1; on the other hand, the material properties were fine-tuned in the Analysis-2. The comparison of the force-displacement curves between the numerical analysis and the static indentation experiment is presented in Fig.5 and two kinds of the analysis result are also shown in Fig. 5.
As shown in Fig. 5 and Table 4, it is seen that the tendency of the force-displacement curves are relatively the same and specially the maximum force in Analysis-2 is good agreement with the experiment results, but different in the force data after the initial maximum force in detail.
There are some reasons why the force data in the numerical analysis is different with the experiment

data. One of the reasons is the material card (*MAT 22) which may be unable to capture transverse impact failures in LS-DYNA as mentioned above. The boundary condition and mesh size should be considered for the more accurate results. A three dimensional solid element also should be used to implement and visualize delamination by the failure mode.
It seems that the fiber breakage may be occurred after the force reached the maximum at 4.39kN in a numerical analysis because in Chang-Chang failure theory the longitudinal tensile strength mainly affects the fiber breakage, and it also affects the maximum force dominantly.

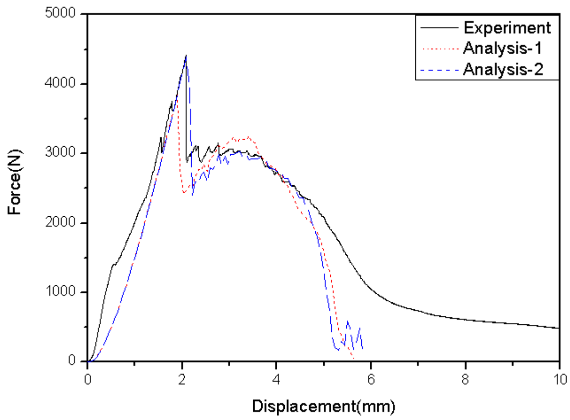

Fig. 5. Comparison of the force-displacement curves between the numerical analysis and the static indentation experiment (2S, D/d=3)

The comparisons of the maximum force and the penetration energy from the static indentation experiments and the numerical analysis are presented in Table 4. The penetration occurred when the indentor reached at 3.8mm downward, so the integration was conducted until the penetration was occurred.

Table 4. Comparison of the maximum force and the penetration energy

2S D/d=3	Maximum Force(N)	Penetration energy (J)
Experiment	4,420	9.64
Analysis-1	3,850	8.56
Analysis-2	4,390	8.69

The stress distribution on the specimen in the numerical analysis is shown in Fig. 6.

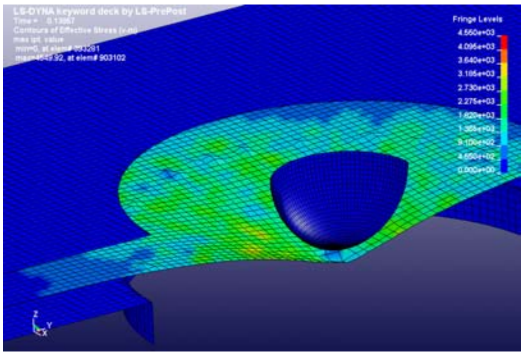

Fig. 6. Stress distribution on the specimen

5 Conclusions

In this study, the static indentation experiment was conducted and the force-displacement curve which was used to calculate the penetration energy was obtained. The high-velocity impact experiment was also conducted and the absorbed energy was calculated using the initial velocity right before the penetration and the residual velocity after the penetration. The numerical model was used to simulate the behavior of the composite laminates by the quasi-static load. The results from the numerical analysis were agreed well with the results from the static indentation experiment.
Furthermore, it is necessary to improve the model considering the effect of boundary condition and mechanical properties depend on the strain rate.

References

[1] I. Kim, S. Hah, M. Jang, and S. Lee "Detection and characterization of high-velocity impact damage in composite laminates using smart sensor signals". *ICCM 17*, 2009.

[2] P.J. Hazell, A. Cowie, G. Kister, C. Stennett, and G. A. Cooper "Penetration of a woven CFRP laminate by a high velocity steel sphere impacting at velocities of up to 1875m/s". *Int. J. Impact Engineering*, Vol. 36, pp 1136-1142, 2009.

[3] C. T. Sun and S. V. Potti "A simple model to predict residual velocities of thick composite laminates subjected to high velocity impact". *Int. J .Impact Engineering*, Vol. 18, pp 339-353, 1996.

[4] S. Ha "*Comparison between static indentation and impact behavior of composite laminates*". A Master's Thesis, Graduate School, Chungnam National University, 2011.

[5] Chian-Fong Yen "Ballistic impact modeling of composite materials". *7th International LS-DYNA Users Conference*, 2002.

[6] J.O. Hallquist, "*LS-DYNA theory manual*", Livermore Software and Technology Corporation, Livermore CA, March 2006.